Democratizing Optometric Care: A Vision-Based, Data-Driven Approach to Automatic Refractive Error Measurement for Vision Screening

Tiffany C.K. Kwok*, Naomi C.M Shum, Grace Ngai* and Hong Va Leong*
CHILab, Department of Computing

Grace Amy Tseng, Hoi-yi Choi, Ka-yan Mak and Chi-Wai Do*
School of Optometry

Hong Kong Polytechnic University, Kowloon, HONG KONG
*Corresponding Authors: tiffany.ck.kwok@connect.polyu.hk, {grace.ngai, hong.va.leong, chi-wai.do}@polyu.edu.hk

***Abstract*— We present a vision-based, data-driven approach to identifying and measuring refractive errors in human subjects with low-cost, easily available equipment and no specialist training. Vision problems, such as refractive error (e.g. nearsightedness, astigmatism, etc) are common ocular problems, which, if uncorrected, may lead to serious visual impairment. The diagnosis of such defects conventionally requires expensive specialist equipment and trained personnel, which is a barrier in many parts of the developing world. Our approach aims to democratize optometric care by utilizing the computational power inherent in consumer-grade devices and the advances made possible by multimedia computing. We present results that show our system is able to match and outperform state-of-the-art medical devices under certain conditions.**

Keywords: *computer-aided diagnosis, vision screening, smartphone refraction, refractive errors*

I. INTRODUCTION

Our pair of eyes, which are also called windows to the soul, are often considered as one of the most, if not the most, important organs in the human body for penetrating and perceiving information. The sense of sight is highly developed in primates and in human beings, over 30% of the brain cortex is devoted to vision processing, as compared with only 8% for touch and 3% for hearing [1][2]. The sense of sight has only become more important with the advent of the information age, as the vast majority of information is designed to be understood and processed through vision.

Given the importance of vision to human perception, it is not surprising that ocular health is of paramount concern nowadays. In many developed regions, such as Hong Kong, vision screening is provided for preschool children as young as 4 years old [3].

Of the commonly-encountered visual problems, uncorrected refractive errors are the leading cause of visual impairment worldwide. Myopia (or nearsightedness), hyperopia (or farsightedness) and astigmatism are the most common conditions, accounting for 43% of visual impairment globally. In Hong Kong, about 80% of young adults are nearsighted [4], [5]. Even though these problems are easily corrected, uncorrected refractive error, especially for those who have high myopia, may result in serious visual impairment or blindness if it is not corrected timely and properly. Indeed, refractive errors constitute one of the leading cause of treatable blindness worldwide, accounting for over 40% of global vision impairment. [6][7].

In developed countries, vision health and refractive error is something that is often taken for granted. However, even in Hong Kong, which has a GDP that easily places the region within the world's top ten *countries*, the supply of trained optometrists does not meet demand [8], almost 80 per cent of employers reporting that employees are difficult to find. It can be easily imagined that the situation in many other places, especially in developing countries, is much worse. Even though the process of diagnosing refractive error has been automated to a certain extent with the development of sophisticated ophthalmic instruments, the cost of these instruments is prohibitive for non-professionals, and the usage of these instruments also requires specialist training.

Our objective is to address this challenge through recent advances in computing and multimedia technology. Today's consumer devices, such as smartphones and tablets, possess computational power that would be unthinkable just several years ago, and recent advances in HCI and usability have rendered these devices easily usable, even by people who have never seen or used a computer before.

The goal and main contribution of our project is the design and evaluation of an automated system that even untrained individuals can use to diagnose refractive error in patients. We will demonstrate that our system produces results that are well within the range of acceptability for vision screening, with minimal human intervention and no specialist expertise needed. To this end, we (1) explore the potential of using consumer-grade mobile devices for screening and detecting photorefractive errors; (2) investigate the extensibility of a current state-of-the-art photorefractive technique for use in these devices; and (3) identify features that can be reliably extracted to train a system for measuring refractive errors.

II. BACKGROUND AND RELATED WORK

Refractive errors refer to the inabilities of the eyes to focus on the visual images from the outside environment [9], which results in blurred vision, or, in more severe cases, serious visual impairment or even blindness. There are four major types of refractive errors: Myopia, Hyperopia, Astigmatism and Presbyopia. The World Health Organization estimates that 153 million people in the world

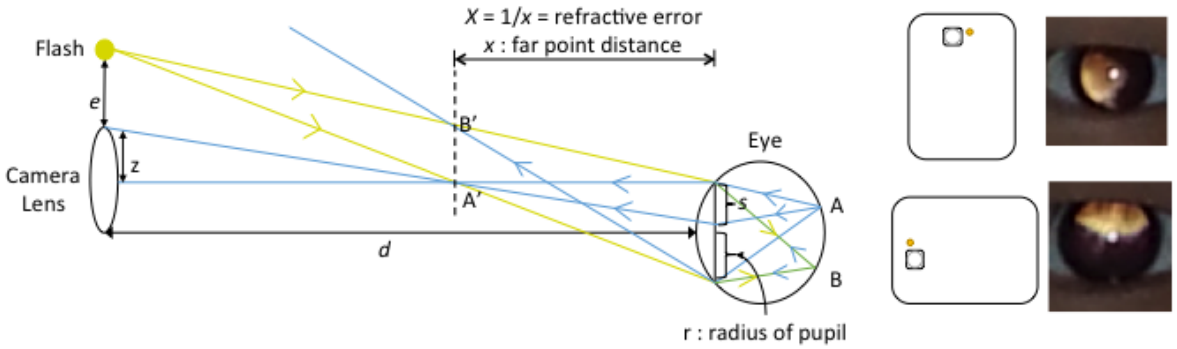

Figure 1 Photorefraction. A flash source is positioned at a distance *e* above the camera lens. *d* is the distance from the lens to the eye being tested. Light enters the myopic eye and is focused in front of the retina. Image AB is formed on the retina and forms an aerial image B'A' at the far point plane of the eye. If the eye is sufficiently myopic, the light returning from this image will enter the camera lens and manifests as a crescent-shaped reflex (*z*) on the camera film/sensor. The photograph of the eye shows a crescent on the same side as the light source (top photo: vertical orientation of mobile device with flash to the left of the eye; bottom photo: horizontal orientation with flash to the top of the eye.) (Ray diagram adapted from Chan, Edwards and Brown [18])

suffer from visual impairment due to uncorrected refractive errors, with eight million blind as a result [10].

We focus on detecting myopia in this project. Myopia, or nearsightedness, is the most prevalent visual disorder resulting from refractive errors, and is estimated to affect as much as 70–90% of the population in Asian countries and 30–40% in Europe and the United States [11].

There are several ways of measuring refractive error. The conventional method uses a phoropter in conjunction with an eye chart. A phoropter contains different lenses [12], which are changed by the optometrist in response to patient feedback [13]. It provides accurate measurements but is expensive and bulky, and can only be operated by trained professionals. It also requires subjective responses from the patient, which presupposes a certain degree of attention and knowledge, which may not be realistic with small children and illiterate individuals.

To eliminate the need for patient response, retinoscopy is a common method of measuring refractive error [14]. A stream of light is projected into the pupil by a qualified optometrist. The light reflex of the pupil is viewed through a retinoscope and the refractive error is determined by the movement and orientation of the reflex.

Another mode of measuring refractive error without the need for patient response is the automated refractor, which analyzes the changes of light as it enters the eye, and uses that to provide an objective measurement of refractive error [15] with high accuracy and without subjective responses. However, it is still a large-sized, expensive machine that requires expert knowledge to operate.

There have been efforts into using computers and image processing techniques for automatic diagnosis of refractive errors without the need for trained professionals. Photorefraction is an objective photographic technique which considers the appearance of the photorefractive reflex of the eye towards a flash of light [16][17]. It has been demonstrated to provide acceptable performance without the need for trained individuals. Chan, Edwards and Brown [18] show that 98% of cases can be diagnosed with a refractive error within 1.0 diopter of that measured by retinoscopy, using photos taken by a single-lens-reflex (SLR) camera and interpreted by trained laypersons. The MTI PhotoScreener [19] has a unique focusing system and flashing fixation light to assure accuracy. It produces results instantly on high speed Polaroid film for interpretation by trained laypersons.

Taking another approach, Eenwyk, Agah, Giangiacomo & Cibis [20] measure refractive error via eye movements. A video recording system captures the image of the foveating eyes both on-axis and slightly off-axis at 30 frames per second. Motion analysis is then used to measure the refractive error in an approach similar to retinoscopy. They achieved 77% accuracy using a decision tree to decide whether the patient should be referred for additional vision screening..

III. Methodology

A. *Photorefraction and Optical Principles*

Our system employs the photorefractive approach with the graphical calibration method developed by Chan, Edwards and Brown [18].

Figure 1 illustrates the optical mechanics. If a patient has refractive error, the photographic reflex of the eye towards a flash of light, which is essentially the reflection of the light off the retina, manifests itself as a crescent in the photograph. The position of the crescent shows whether a patient has hyperopia or myopia. In myopic cases, the eye is focused in front of the light flash, producing a crescent that appears on the same side as the light source. The opposite is true for hyperopic cases, where the crescent appears on the opposite side of the eye [21].

Given the existence of a crescent, the refractive error for myopia can be computed as follows:

$$X = \frac{e}{[d(2r - z)]} + \frac{1}{d}$$

where:

- X = Refractive error
- d = Distance from camera lens to eye
- e = Eccentricity of flash
- 2r = Diameter of the pupil
- z = Size (width) of the refractive reflex crescent

B. Data Acquisition

Since the ultimate objective of our project is to create a system that would not require expensive equipment, or the input or judgement of a trained operator, our experimental data is collected on mobile devices. This is critical as there is a significant difference in quality between photos taken on specialized equipment or even single-lens reflex cameras and those taken with mobile devices.

1) Mobile Application for Data Collection

To ensure the correctness of the collected data, a mobile application was developed to wrap around the camera on an Android device. The objective of the application is to ensure that the photos are taken with the correct flash and orientation configuration.

To prevent distortion of pupil size and crescent size, the camera needs to be aligned along the vertical axis, with as little inclination as possible. The asymmetric nature of refractive error also requires two photographs for each eye, with the flash positioned vertically and horizontally parallel to the camera lens. Our data collection application therefore uses the built-in gyroscope of the phone to detect its position and orientation, and directs the operator to rotate the phone until the flash is at the correct position relative to the lens, whereupon the needed photographs will be taken.

The principle behind photorefraction relies on the reflection of the light source off the subject's retina, which is also the cause of the "red-eye" phenomenon in flash photographs. Since the red-eye reduction feature built into many cameras would constrict the pupils and prevent this phenomenon from occurring, the application turns off this feature and produces a single flash as the shutter is pressed.

The application is installed on a Samsung Galaxy Note II with a 8.0 Mega-pixel Auto Focus Camera. The photographs are taken at the standard 1280x720 pixels.

2) Calibration Eyeglasses

The calculation of the refractive error is based on the size of the pupil and the refractive reflex crescent. It is imperative that the actual size of the pupil is known in order to obtain an accurate computation.

To achieve this, we insert calibration points that are designed to be clearly visible and easily recognizable. If the actual distance between the calibration points is known, the actual size of the iris, pupil and crescent can be estimated by comparing their size with the distance between the calibration points.

The eyeglass frames in Figure 2 were used for calibration. Two reflective stickers are affixed onto the frame, which is then worn by the subject while the photos are taken. The frame is specially chosen to be as unobtrusive as possible, with the main part being made of thin metal and the rest of the frame from nylon wire, to avoid potential problems with occlusion.

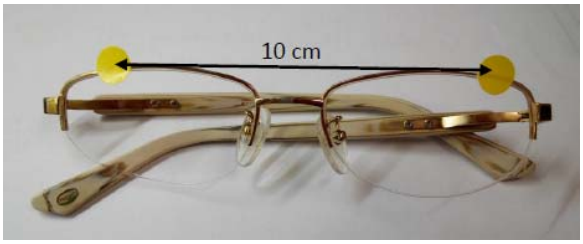

Figure 2 Eyeglass Frames for Calibration.

3) Data Collection

The data was collected in an optometry clinic. Subjects were asked to remove their corrective lenses (glasses or contact lenses) and a state-of-the-art autorefractor (Grand Seiko Auto Ref/Keratometer WAM-5500) is first used to measure the refractive error of both eyes. This equipment is certified for medical use, and is capable of producing highly-accurate measurements.

The photos were taken with the lights dimmed. The subject sits in an optical chair and the mobile device is placed 1 meter away. A tripod is used to keep the device steady and adjusted such that the camera lens is at the level of the subject's eyes. The subjects are asked to focus on the device (as best as they can without corrective lenses), and 4 photos are taken: 2 photos with the device in a horizontal position and 2 photos in a vertical orientation.

C. Data Processing and Feature Extraction

1) Feature Detection and Measurement

Once the data has been acquired, the needed features are identified and measured. Our system uses IntraFace [22] to identify the region of the eyes on the face. The two calibration points are identified with Hough Circle Transform to detect collinear sets of points in an image (Figure 3). The distance between the center of the two points is then used to calculate the actual size of the eye features.

Figure 3 Identified calibration points on subject's face.

To locate the crescent, we first apply inverted thresholding to amplify the bright and dark contrast into black and white, thus enhancing the boundary of the crescent. Canny Edge Detection [23] is then applied to identify contours in the image.

The inverted thresholding and edge detection works well to identify the crescent, but locating the pupil is more difficult. For many of our subjects with dark eyes, the pupil cannot be readily located in the photo due to its blurred boundary, and its color similarity with the iris. To solve this challenge, the pupil is identified with respect to the location of the reflective reflex crescent. We make the simplifying assumption that the shape of the pupil is circular. As the crescent is produced by the light reflecting from the retina inside the eye, it must necessarily be enclosed by the pupil. Furthermore, its outer boundary is delineated by the boundary of the pupil. The boundary of the pupil can therefore be reconstructed by fitting a circle onto the arc identified as the outer boundary of the crescent. (Figure 4)

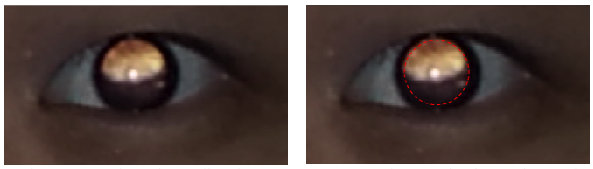

Figure 4 Using the reflective crescent to estimate the boundary of the pupil. The boundary between pupil and iris is hard to determine in subjects with dark eyes (left). The boundary of the pupil can be reconstructed by fitting a circle onto the arc identified as the outer boundary of the crescent (right).

2) Automatically Determining Detection Failures

Our process works well for the majority of the cases, but there is always a possibility of detection failure. Given the nature of our application, it is imperative that the system be able to automatically determine when it has failed to detect the needed features and alert the operator as needed. In addition, it is better to err on the conservative side and report a failure when there is none, rather than to mistakenly identify a feature and use the wrong data in the computation (e.g. Type 1 errors are preferable to Type 2 errors).

An inspection of the results reveals several causes of detection failure. For example, other parts of the photo may be inaccurately identified as the face or eye (Figure 5). In addition, as the eye itself takes up only a very small fraction of the whole photo, the intra-eye features, such as the contours, may not be accurately identified.

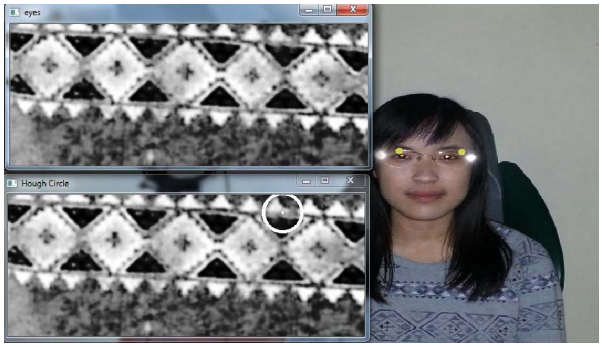

Figure 5 Example of detection failure – the "eye", as detected by the system (circled) is actually part of the subject's sweater.)

Our system uses heuristics to identify certain potentially problematic cases. These include: failure to identify contours; the crescent size computed as larger than the pupil size; pupil size larger than iris size, crescent size too small, or a too-large refractive error. In these cases, the operator will be prompted to assist the system. Depending on the detected failure, the operator is either asked to identify the corners of a given eye, or to draw a rectangle (by marking the opposite corners) that encloses the eye region. This is the limit of user input into the process and clearly does not require any specialist expertise.

In our experiments, 19% of the cases were identified as potential detection failures. Of these cases, 89% of them were real detection failures, and the needed features were successfully recovered after the manual operator input. Of the remaining 81% of the cases, 11.5% of them should have been flagged as detection failures but were not flagged as such by the system.

IV. Evaluation Results

Our system is evaluated based on the correctness of the refractive error computed. The measurement from the autorefractor is taken as the gold standard, and we evaluate the performance via the mean absolute error between the refractive error calculated by our system and the measurement from the autorefractor.

We experiment with two methods of calculating the refractive error. The first method, which we shall term *theory-driven*, uses the formula proposed by Chan et al [18]. The second method, which we term *data-driven*, trains a Support Vector Regression (SVR) [24] machine with part of the data and uses the trained model to compute the refractive error for the remaining held out test data. We use the WEKA [25] package for our SVR and the size of the crescent, pupil and iris were used as features. Leave-one-out cross validation was used to evaluate across the whole data set, training with all but one of the instances on each iteration and testing on the final instance. The final performance is the average across all iterations.

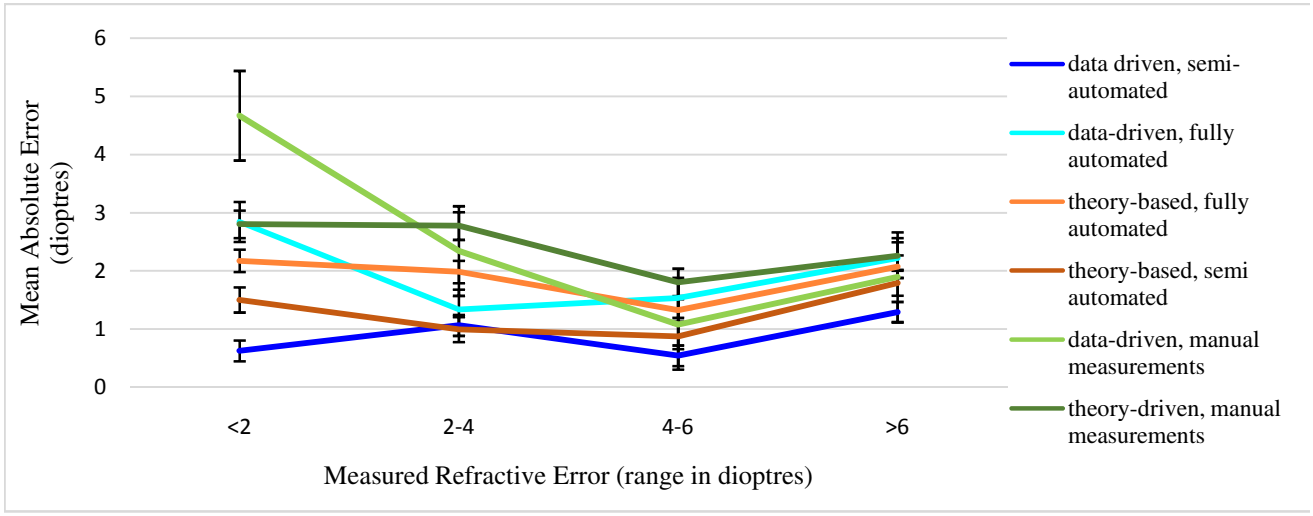

Figure 6:Relationship between measured refractive error and mean absolute error.

We also evaluate the impact of our detection failure process. The *fully automated* method relies wholly on the system to detect the eye features; therefore erroneously identified eye regions will result in wrongly measured features. (A failure to detect the eye altogether results in the instance being dropped from the data set.) The *semi-automated* method incorporates failure detection and prompts for operator input when problematic cases are identified.

To get a sense of the difficulty and ambiguity of the task, 3 optometry students were invited to manually measure the size of the eye features from the acquired data. These students possess substantive background in the discipline and are familiar with the underlying theories and structures. Since there will be some deviation between the measurements arrived at by the three individuals, we take the average of their figures as the correct measurement for the *manual* method.

48 people were invited to take part in our experiments, giving us 96 instances (1 instance = 1 eye) in total. The operator for the data acquisition process was an undergraduate Computer Science student with no background in optometry or health sciences.

Table 1 shows the results. The range of refractive error that can be measured by our system ranges between 0.75 diopters and 13.62 diopters.

Table 1: Experimental Results

		Mean Absolute Error between calculated refractive error and gold standard (diopters)	
		Theory-driven	**Data-driven**
Feature Identification and / or Measurement	**Fully-Automated**	1.9174	1.6477
	Semi-Automated	1.1422	**0.9832**
	Manual	2.3096	1.9651

The theory-driven model achieves a mean absolute error of 1.9 diopters when using the fully-automatically-measured data for calculations. This performance improves to an error of 1.14 diopters when minimal operator intervention is applied to correct for obvious errors. This improvement in performance is obviously due to the errors introduced when the eye features are wrongly detected and illustrates the contribution of our failure detection process.

Taking the data-driven approach, the SVR achieves better overall performance both with and without failure detection. When failure detection and operator intervention is integrated, the mean absolute error drops to less than 1 diopter, which is within the range of error of the commercial autorefractor, and well within the limits of acceptability for vision screening.

There are several possible reasons for the less satisfactory performance of the theory-driven method. First, the formula was derived on an idealized setup that uses a SLR camera taking photos onto film. SLR cameras are known to take better pictures than the cameras on mobile devices, and the medium of film suffers less from quantization and pixelization, compared with digital devices. Second, the position of the flash light source may also pose a problem. The "eccentricity" of the flash is difficult to calculate or measure in mobile devices, where the flash bulb and the lens are close together, especially when compared with the external flash mount used in many SLR cameras.

Interestingly, the performance achieved with the manual measurements result in a larger error regardless of the method used to calculate the refractive error. This illustrates the difficulty of the task: the lower resolution of the mobile device photos (compared with the SLR cameras used in the original work) makes it hard for even trained specialists to determine the measurements of the needed features. The color similarity between the iris and the pupil also posed a problem: in many cases, the students reported that it was not easy to identify the pupil boundary.

Figure 6 shows the relationship between the measured refractive error and the mean absolute error. Across all methods, it can be seen that the mean absolute error tends to increase with the measured refractive error. It can also be seen that our data-driven SVR approach with failure detection (semi-automated) outperforms the rest of the methods at all refractive error levels.

V. Conclusion and Future Development

This paper presents a vision-based, data-driven approach to automatically measuring refractive errors with minimal operator input. Our system uses only a standard mobile device and the embedded camera, and is successful at detecting and measuring myopia with less than 1.0 diopter of error. Some manual correction is required, but it takes no special expertise or training (beyond being able to read instructions and operate a mobile device), and only 19% of data requires this additional manual processing.

For future development, we plan to investigate the impact of the form factor of the mobile device on the model. This will allow us to generalize our system to other devices, including newer devices in which the flash source is not aligned with the camera lens, or even with multiple flash sources in different colors. We also plan to extend our system to diagnose hyperopia and other refractive errors that can be detected using photorefraction.

References

[1] D. C. Van Essen, "Organization of Visual Areas in Macaque and Human Cerebral Cortex," Vis. Neurosci., vol. 1, pp. 507–521, 2004.

[2] D. C. Van Essen and H. A. Drury, "Structural and Functional Analyses of Human Cerebral Cortex using a Surface-based Atlas," J. Neurosci., vol. 17, no. 18, pp. 7079–7102, 1997.

[3] Pre-School Vision Screening. Family Health Service, Department of Health, The Government of the Hong Kong Special Administrative Region.

[4] "Visual Impairment and Blindness," World Health Organization, 2014. [Online]. Available: http://www.who.int/mediacentre/factsheets/fs282/en/.

[5] D. Pascolini and S. P. Mariotti, "Global Data on Visual Impairment:2010," British Journal Ophthalmology, 2011. [Online]. Available: http://www.who.int/blindness/publications/globaldata/en/.

[6] J. Khan, "A million life changing moments," Optometry Today, 2014. [Online]. Available: http://www.optometry.co.uk/news-and-features/features/?article=6417.

[7] R. Dandona and L. Dandona, "Refractive Error Blindness," Bull. World Health Organ., vol. 79, no. 3, pp. 237–243, 2001.

[8] J. Tam, "Hong Kong's eye doctors question vision of training so few in profession," South China Morning Post, 2013. [Online]. Available: http://www.scmp.com/news/hong-kong/article/1323000/hong-kongs-eye-doctors-question-vision-training-so-few-profession.

[9] "What is a refractive error?," World Health Organization, 2013. [Online]. Available: http://www.who.int/features/qa/45/en/.

[10] S. Resnikoff, D. Pascolini, S. P. Mariotti, and G. P. Pokharel, "Global magnitude of visual impairment caused by uncorrected refractive errors in 2004," Bull. World Health Organ., vol. 86, no. 1, pp. 1–80, 2008.

[11] D. R. Fredrick, Clinical Review□: Myopia, vol. 324. 2002, pp. 1195–1199.

[12] G. L. Campbell, Phoroptors, Early American Instruments of Refraction, and Those Who Used Them. Wheaton, Illinois, 2008.

[13] L. Twisselmann, "Phoropter," U.S. Patent 5223864 A, 1993.

[14] F. W. Jobe, "Retinoscope," U.S. Patent 2,715,352, 1955.

[15] D. L. Rogers, D. E. Neely, J. B. Chapman, D. A. Plager, D. T. Sprunger, N. Sondhi, G. J. Roberts, and S. Ofner, "Comparison of the MTI Photoscreener and the Welch-Allyn SureSightTM autorefractor in a tertiary care center," J. Am. Assoc. Pediatr. Ophthalmol. Strabismus, vol. 12, no. 1, pp. 77–82, 2008.

[16] D. O. Bixler, "Eye Care for Infants and Young Children," in Electrodiagnostics, Ultrasound, Neuroimaging and Photorefraction, Butterworth-Heinemann, 1997, pp. 114–117.

[17] H. Howland, "The optics of static photographic skiascopy. Comments on a paper by K. Kaakinen: A simple method for screening of children with strabismus, anisometropia or ametropia by simultaneous photography of the corneal and the fundus reflexes.," Acta Ophthalmol., vol. 58, no. 2, pp. 221–7, 1980.

[18] O. Y. C. Chan, M. Edwards, and B. Brown, "Calibration and Validity of an Eccentric Photorefractor," Ophthal. Physiol. Opt., vol. 16, no. 3, pp. 203–210, 1996.

[19] F. Weinand, M. Graf, and K. Demming, "Sensitivity of the MTI Photoscreener for Amblyogenic Factors in Infancy and Early Childhood," Graefe's Arch. Clin. Exp. Ophthalmol., vol. 236, no. 11, pp. 801–805, 1998.

[20] J. V. Eenwyk, A. Agah, J. Giangiacomo, and G. Cibis, "Artificial Intelligence Techniques for Automatic Screening of Amblyogenic Factors," Trans. Am. Ophthalmol. Soc., vol. 106, pp. 64–74, 2008.

[21] A. Roorda and M. C. W. Campbell, "Slope-based Eccentric Photorefraction: Theoretical Analysis of different Light Source Configurations and Effects of Ocular Aberrations," J. Opt. Soc. Am. A, vol. 14, no. 10, pp. 2547 – 2556, 1997.

[22] X. Xiong and F. D. la Torre, "Supervised Descent Method and its Applications to Face Alignment," in EEE Conference on Computer Vision and Pattern Recognition (CVPR), 2013.

[23] J. Canny, "A Computational Approach to Edge Detection," IEEE Trans. Pattern Anal. Mach. Intell., vol. 8, no. 6, pp. 679–698, 1986.

[24] H. Drucker, C. J. C. Burges, L. Kaufman, A. J. Smola, and V. N. Vapnik, Support Vector Regression Machines. MIT Press, 1996.

[25] M. Hall, E. Frank, G. Holmes, and B. Pfahringer, "The WEKA Data Mining Software: An Update," SIGKDD Explor. Newsl., vol. 11, no. 1, pp. 10–18, 2009.

.